

differential cross sections are insensitive to the detailed shapes of the radial wave functions. Experimentally, this was demonstrated by the fact that the angular distributions of levels of a given spin and parity are quite similar to each other for angles less than 60° . The angular distributions are sensitive only to the angular-momentum transfer, so that reliable spin and parity assignments can be made. The magnitude of the cross section contains dynamical information about the excited states. By the use of the vibrational model, electromagnetic rates have been deduced and compared with theoretical predictions.

Using the procedures mentioned above, we have made spin and parity assignments to a number of states, and have measured their transition rates.⁵⁸ Several 2^+

⁵⁸ *Note added in proof.* The values of the inferred electromagnetic transition rates in Weisskopf units were derived from a formula based on the vibration of a sharp-edge charge distribution whose radius is taken to be $1.2 A^{1/3}$. Because the higher multipolarities strongly weight the surface region, the magnitudes are underestimated. If the measured Fermi-type charge distribution is used, then the transition rates for $E3$, $E4$, and $E5$ transitions would be multiplied by approximately 1.4, 2.1, and 3.3, respectively. These numbers are sensitive to the parameters of the charge distribution and therefore contain an uncertainty which is difficult to estimate. However, there is some evidence that this increase is

states in $\text{Ca}^{40,42}$ are in reasonable agreement with the results of Gerace and Green.³⁹ In addition, we have observed a 4^+ doublet between 6 and 8.5 MeV in $\text{Ca}^{40,42,48}$ which appears to be a core excitation. The number of 3^- states and the variation of 3^- and 5^- strength with mass number are not readily explained by our present ideas based on the particle-hole model.

ACKNOWLEDGMENTS

It is a pleasure to acknowledge the contribution of N. S. Wall, who designed the external beam system. We would like to thank T. A. Belote, W. J. Kossler, J. Alster, N. S. Wall, and E. F. White for valuable criticisms of the manuscript. The assistance of the cyclotron staff of E. F. White, F. Fay, and J. Byrne was extremely valuable. We would like to thank W. Gerace, T. T. Kuo, A. M. Green, and R. J. Peterson for communicating their results before publication. The programming assistance of T. Provost is gratefully acknowledged.

experimentally required when comparing electromagnetically measured $E3$ values in light nuclei with those deduced from inelastic scattering experiments. It should be noted that the values of β_λ and the relative values of G_λ given in the tables are not altered by this procedure.

Positron Decay of $\text{Mg}^{22\dagger}$

A. GALLMANN AND G. FRICK

Institut de Recherches Nucléaires, Strasbourg, France

AND

E. K. WARBURTON

Brookhaven National Laboratory, Upton, New York

and

Institut de Recherches Nucléaires, Strasbourg, France

AND

D. E. ALBURGER AND S. HECHTL

Brookhaven National Laboratory, Upton, New York

(Received 16 March 1967; revised manuscript received 24 July 1967)

The positron decay of Mg^{22} to excited states of Na^{22} was investigated using the $\text{Ne}^{20}(\text{He}^3, n)\text{Mg}^{22}$ reaction to form Mg^{22} . The relative cross section for the $\text{Ne}^{20}(\text{He}^3, n)\text{Mg}^{22}(\beta^+)\text{Na}^{22}$ reaction was measured as a function of He^3 energy for He^3 energies between 2.0 and 5.0 MeV. A half-life of 4.03 ± 0.05 sec was obtained for Mg^{22} . In addition to the main positron branches to the Na^{22} 0.657- and 0.583-MeV levels, which were measured to be $(59 \pm 6)\%$ and $(36 \pm 6)\%$, respectively, a branch of $(5.1 \pm 0.4)\%$ was observed leading to the 1.937-MeV level of Na^{22} . The $\log ft$ for this branch is 3.55 ± 0.04 , which establishes the 1.937-MeV level as 1^+ . Upper limits were placed on positron branches to all other excited states of Na^{22} below an excitation energy of 3.6 MeV. The $0.657 \rightarrow 0.583$ transition in Na^{22} was found to have an energy of 73.9 ± 0.1 keV. An incidental result was a value of 472.3 ± 0.1 keV for the energy of the γ -ray transition from the isomeric first-excited state of Na^{24} .

I. INTRODUCTION

THE isotope Mg^{22} has a mass excess of 4.835 ± 0.020 MeV with respect to Na^{22} and decays to the latter by positron emission.¹⁻⁶ Since the nucleus Mg^{22} is even-

even, and therefore can be safely assumed to have a spin of 0^+ , the positron transition to the 3^+ ground

[†] Work at Brookhaven National Laboratory performed under the auspices of the U. S. Atomic Energy Commission.

¹ R. W. Kavanagh, *Bull. Am. Phys. Soc.* **7**, 462 (1962).

² P. M. Endt and C. Van der Leun, *Nucl. Phys.* **34**, 1 (1962).

³ R. E. Benenson and I. J. Taylor, *Bull. Am. Phys. Soc.* **11**, 737 (1966).

⁴ J. Cerny, S. W. Cosper, G. W. Butler, R. H. Pehl, F. S. Goulding, D. A. Landis, and C. Détraz, *Phys. Rev. Letters* **16**, 469 (1966).

⁵ P. H. Barker, N. Drvdsdale, and W. R. Phillips, *Proc. Phys. Soc. (London)* **91**, 587 (1967).

⁶ The mass excess of Mg^{22} used throughout this work is a weighted average of the values given in Refs. 4 and 5 and the two values quoted in footnote 10 of Ref. 4. This average is $-(347 \pm 20)$ keV on the C^{12} scale.

state of Na^{22} is second-forbidden and is not observed. Allowed positron transitions can take place to the 1^+ first excited state of Na^{22} at 0.583 MeV, to the 0^+ second excited state at 0.657 MeV, and perhaps to higher excited states. The transition to the 0^+ level is super-allowed and is therefore the most probable. This latter level cascades 100% through the state at 0.583 MeV with the emission of γ rays with energies of 73.9 ± 0.1 keV (present work) and 583.04 ± 0.10 keV.⁷

The β^+ activity of Mg^{22} was first observed by Kavanagh¹ who produced the isotope by means of the reaction $Ne^{20}(He^3, n)Mg^{22}$ at $E_{He^3} = 3$ MeV. He observed γ rays with energies of 73.5 ± 0.8 keV and 586 ± 6 keV, which he assigned to the cascade decay of the 0.657-MeV level of Na^{22} . By measuring the decay of the 74-keV line a half-life of 3.94 ± 0.10 sec was obtained. Benenson and Taylor³ repeated the same experiment and obtained a value of 3.9 ± 0.1 sec for the Mg^{22} half-life from observations of the decay of the 0.583-MeV γ ray. Recently, Barker, Drysdale, and Phillips⁵ have also examined the $Ne^{20}(He^3, n)Mg^{22}(\beta^+)Na^{22}$ reaction. They obtained a half-life of 3.99 ± 0.12 sec and found β branches to the 0.657-MeV level (59 ± 2)% and to the 0.583-MeV level (41 ± 2)%.

We have also investigated the positron decay of Mg^{22} using the $Ne^{20}(He^3, n)Mg^{22}$ reaction. Our main efforts were to remeasure the half-life of Mg^{22} , of check the positron branching intensities to the 0.657- and 0.583-MeV levels, and to search for positron transitions to higher states of Na^{22} .

II. THE HALF-LIFE OF Mg^{22}

Our work on the positron decay of Mg^{22} was commenced using the 5.5-MV accelerator at the Centre de Recherches Nucléaires at Strasbourg. The isotope Mg^{22} was produced by the bombardment of natural neon gas (90.9% Ne^{20} , 0.3% Ne^{21} , 8.8% Ne^{22}) with He^{3+} ions. The gas was confined at a pressure of ~ 1 atm. The beam entered the gas volume through a 0.0001-in.-thick Ni foil, traversed 2 cm of the gas and was stopped in a Ta disk. The energy losses of 5.5-MeV He^3 ions in the Ni foil and the gas volume were 780 and ~ 900 keV, respectively.

Several Ge(Li) detectors, all having been prepared at Strasbourg, were used for γ -ray detection. The final results for the half-life were obtained with a 10-cc plane-drifted detector which had a resolution [full-width-at-half maximum (FWHM)] of 9.5 keV for the 1.17-MeV γ rays of Co^{60} . The Ge(Li) detector was placed at 90° to the beam with the front face 3.5 cm from the gas volume. It was shielded on its sides by lead.

The method used to study the delayed γ rays from Mg^{22} was to bombard the gas target for a time t_1 and then to intercept the beam far from the target and

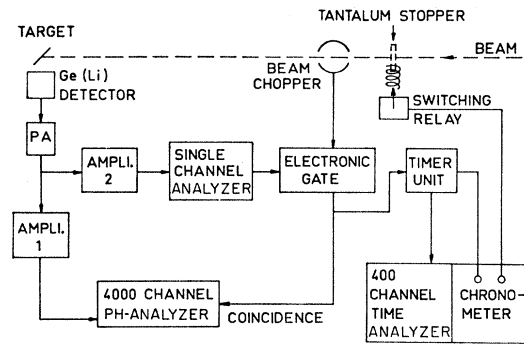


FIG. 1. Block diagram of the electronic circuits used in the experiments at Strasbourg.

count the γ rays for a time t_2 . This procedure was automatically recycled until sufficient statistics were accumulated. The electronics illustrated schematically in Fig. 1 were used for this purpose. As shown in Fig. 1, two different mechanical systems were used to intercept the beam. In the first a rotating mechanical chopper, which was placed in the path of the beam gave a 44-msec cycle with equal beam irradiation and delayed counting intervals of 22 msec each. The gating circuit insured that only those pulses occurring during the "beam off" interval were analyzed. This system was used in preliminary studies of the delayed γ -ray spectrum from $Ne^{20}+He^3$. The γ -ray spectrum of Fig. 2 was obtained in this manner as was the yield curve for the 74-keV γ ray, illustrated in Fig. 3. The latter was obtained by recording spectra for a known integrated charge as a function of incident He^3 energy and extracting from each spectrum the intensity of the 74-keV full-energy-loss peak.

The half-life of Mg^{22} was studied using a tantalum beam stopper activated by a switching relay. A cycle consisted of bombarding the target for six half-lives (24 sec) and then intercepting the beam and counting for a given time. A single-channel analyzer selected a narrow band of amplitudes so that only those pulses corresponding to a given γ -ray pulse-height interval were time analyzed. The γ -ray pulses were stored in a 400-channel pulse-height analyzer which was used as a time-channel analyzer. γ -ray spectra were accumulated simultaneously in a 4000-channel pulse-height analyzer.

In Fig. 4 is shown a time decay curve obtained with a gate set on the full-energy-loss peak of the 0.583-MeV γ rays (see Fig. 2) and with a counting time of 72 sec. The decay of the 4-sec Mg^{22} activity is apparent in the first ~ 50 channels (400 msec/channel) of Fig. 4 and has decreased to a negligible amount by channel 75. Activities other than Mg^{22} which can contribute to this decay curve are listed in Tables I and II. $Mg^{23}(\beta^+)Na^{23}$ was the only activity listed in Table I which was not observed. The "background" activity of Fig. 4 is due to the continuum under the 0.583-MeV peak. This continuum arises from bremsstrahlung and from the Compton distributions of higher-energy γ rays. It is apparent from Tables I and II that the time-decay curve of

⁷ E. K. Warburton, J. W. Olness, and A. R. Poletti, Phys. Rev. **160**, 938 (1967); A. R. Poletti, E. K. Warburton, J. W. Olness, and S. Hechtel, *ibid.* **162**, 1040 (1967); E. K. Warburton, A. R. Poletti, and J. W. Olness (to be published).

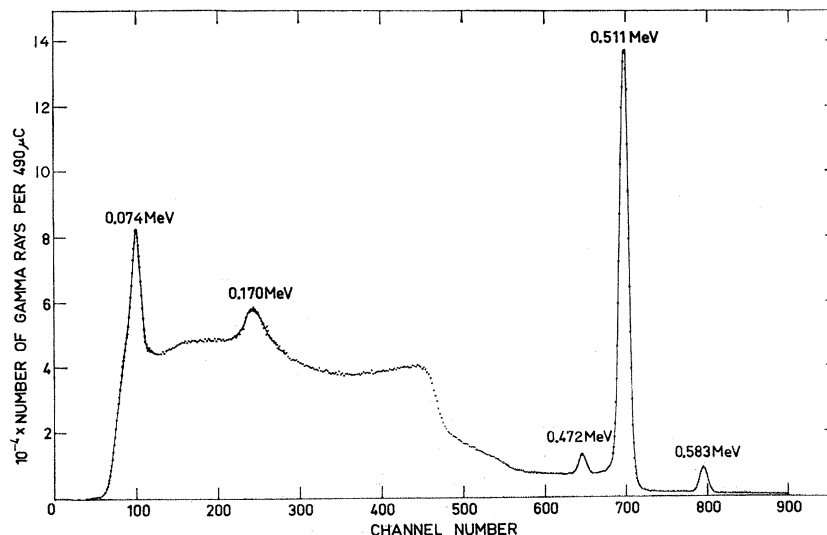


FIG. 2. Spectrum of the low-energy delayed γ rays from the reactions $\text{Ne}^{20} + \text{He}^3$ and $\text{Ne}^{22} + \text{He}^3$ produced by 5.5-MeV He^3 bombardment of a natural Ne target. The 0.511- and 0.170-MeV peaks are the full-energy-loss and back-scattered peaks of annihilation radiation. The 0.583- and 0.074-MeV peaks are due to the positron decay of Mg^{22} , the 0.472-MeV peak is ascribed to the $0.472 \rightarrow 0$ transition in Na^{24} resulting from the $\text{Ne}^{22}(\text{He}^3, p)\text{Na}^{24}$ reaction. Its presence in the delayed spectrum follows from the half-life of 19.6 msec (Ref. 2) for the 0.472-MeV first excited state of Na^{24} . There is an electronic cutoff below channel 60.

Fig. 4 is quite complex; however, the Mg^{22} 4-sec activity and long-lived activities ($T_{1/2} \gg 4$ sec) contribute almost all of the intensity; thus, analysis of Fig. 4 to obtain the Mg^{22} half-life was not unduly complicated. Three decay curves similar to that of Fig. 4 were measured using somewhat different experimental conditions. For all a least-squares fit was made to the data above channel 75 under four assumptions: (1) constant count rate, (2) a count rate decreasing linearly with time, (3) a 17-sec activity plus a constant background, and (4)

a 22.8-sec activity plus a constant background. The functional form so determined was then extrapolated to lower channel numbers and subtracted from the experimental time-decay curve. A least-squares fit was then made to the resultant time spectra assuming a single activity. It was found that the half-lives so obtained were consistent with each other. The weighted average of the three determinations of the Mg^{22} half-life yielded $T_{1/2} = 4.03 \pm 0.05$ sec.

The half-life associated with the 74-keV γ ray (Fig. 2)

TABLE I. Radioactive isotopes produced by the bombardment of a natural neon target by He^3 ions ($E_{\text{He}^3} \leq 7$ MeV).^a

Isotope	Reactions	Q (MeV)	Half-life	Activity	$E_\beta(\text{max})^b$ (MeV)	E_γ (MeV)
Ne^{19}	$\text{Ne}^{20}(\text{He}^3, \alpha)\text{Ne}^{19}$	+3.702	17.8 sec	β^+	2.23 (100%)	...
Na^{21}	$\text{Ne}^{20}(\text{He}^3, d)\text{Na}^{21}$	-3.047	22.8 sec	β^+	2.51 (98%) 2.16 (2%)	...
Na^{22}	$\text{Ne}^{21}(\text{He}^3, t)\text{Na}^{21}$ $\text{Ne}^{20}(\text{He}^3, p)\text{Na}^{22}$	-3.548 +5.784	2.58 yr	β^+	1.82 (0.06%) 0.54 (89.7%) E.C. ^c (10.2%)	...
Na^{24}	$\text{Ne}^{21}(\text{He}^3, d)\text{Na}^{22}$ $\text{Ne}^{22}(\text{He}^3, t)\text{Na}^{22}$ $\text{Mg}^{22}(\beta^+)\text{Na}^{22}$ $\text{Ne}^{22}(\text{He}^3, p)\text{Na}^{24}$	+1.250 -2.860 ... +8.031	14.97 h	β^-	1.40 (~100%)	{ 2.754 1.369
Na^{24m}	$\text{Ne}^{22}(\text{He}^3, p)\text{Na}^{24m}$	+7.558	19.6 msec	γ	...	0.472
Mg^{23}	$\text{Ne}^{21}(\text{He}^3, n)\text{Mg}^{23}$	+6.578	12 sec	β^+	3.06 (91%) 2.62 (9%)	...
Mg^{22}	$\text{Ne}^{20}(\text{He}^3, n)\text{Mg}^{22}$	+0.165	4 sec	β^+	3.16 (59%) 3.23 (41%)	0.439 0.074 0.583

^a From Ref. 2, the present work, and T. Lauritsen and F. Ajzenberg-Selove, in *Nuclear Data Sheets*, compiled by K. Way *et al.* (National Academy of Sciences—National Research Council, Washington 25, D. C., 1962), Sets 5 and 6; F. Ajzenberg-Selove and T. Lauritsen, *Nucl. Phys.* 11, 1 (1959).
^b The % branch corresponding to each decay mode is given in parentheses. The branching ratios for Mg^{22} are from Ref. 5.
^c Electron capture.

TABLE II. Background activities observed in the bombardment of a neon-gas target (nickel window, tantalum beam stop) with He^3 ions ($E_{He^3} \leq 7$ MeV).

Isotope	Source	Half-life	Activity	E_γ (MeV)
K^{40}	Room background	1.28×10^9 yr	E.C. ^a	1.46
ThC''	Room background	2.615
O^{14}	$C^{12}(He^3, n)O^{14}$ ($Q = -1.148$ MeV)	72 sec	β^+	2.313
C^{11b}	$C^{12}(He^3, \alpha)C^{11}$ ($Q = 1.856$ MeV)	20.4 m	β^+	...
Cu^{60}	$Ni^{58}(He^3, \beta)Cu^{60}$ ($Q = 5.629$ MeV)	24 m	β^+	3.12 1.79 1.33 0.82

^a Electron capture.

^b Not observed but presumed present.

was also measured. The result was $T_{1/2} = 3.6 \pm 0.5$ sec, consistent with, but considerably less accurate than, the half-life determined from the 0.583-MeV γ ray. The larger uncertainty is due to the greater relative intensity of the background under the 74-keV line and to poorer statistics.

III. $Mg^{22}(\beta^+)Na^{22}$ BRANCHING RATIOS

The branching-ratio measurements reported in this section were carried out using the 3.5-MV electrostatic accelerator at the Brookhaven National Laboratory.

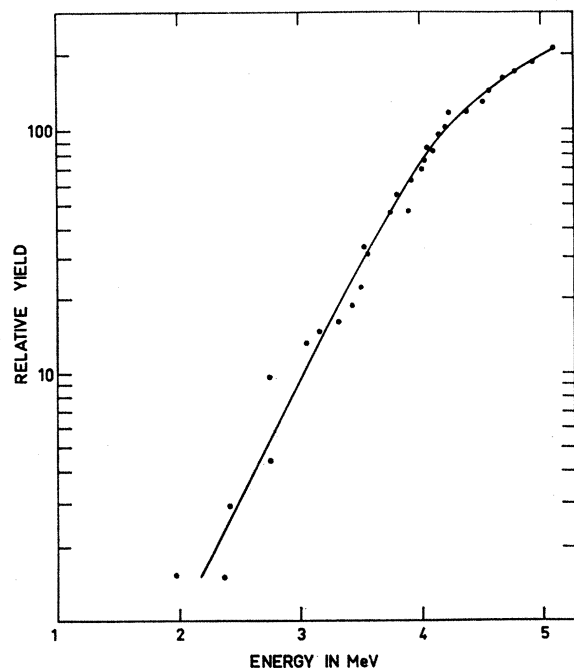


FIG. 3. Relative yield of the 74-keV γ ray from the reaction $Ne^{20}(He^3, n)Mg^{22}(\beta^+)Na^{22}$ as a function of He^3 energy. The solid line is drawn smoothly through the data points. The energies of the data points correspond to the mean He^3 energy in the neon target.

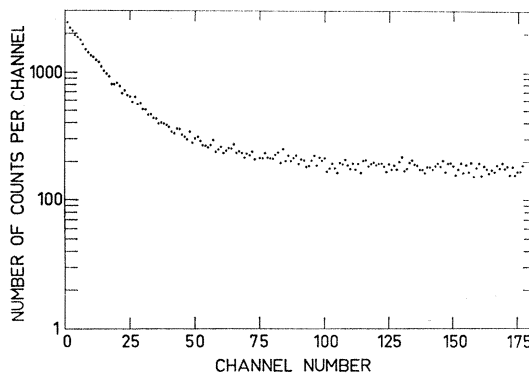


FIG. 4. Time decay of the 583-keV γ rays due to $Mg^{22}(\beta^+)Na^{22}$. The counting time per channel is 400 msec. The ~ 4 -sec Mg^{22} activity is negligible for channel numbers > 75 . The origin of the "background" apparent above channel 75 is discussed in the text.

A. The Na^{22} 0.583-MeV Level

The main decay of Mg^{22} is the super-allowed $0^+ \rightarrow 0^+$ transition to the Na^{22} 0.657-MeV level. It is clear from the energy-level spectrum⁸ of Ne^{22} that no other Na^{22} 0^+ , $T=1$ levels are energetically accessible to positron decay from Mg^{22} [states of Na^{22} with $E_x < (3.82 \pm 0.02)$ MeV so qualify]. However, allowed positron decay could take place to the 0.583-MeV level and to other 1^+ states of Na^{22} . We consider first the possible decay to the 0.583-MeV level which has recently been found⁵ to account for $(41 \pm 2)\%$ of all decays.

The positron branch to the 0.583-MeV level was measured by comparing the intensities of the 583- and 74-keV γ rays using an 8-cc Ge(Li) detector that had been fabricated at Brookhaven by H. W. Kraner. The main difficulty of this method is in obtaining the relative efficiencies for detecting these two γ rays. Bi^{207} is an activity suited to this purpose since it emits a γ ray of 570 keV as well as K_α and K_β x rays with mean energies of 74.2 and 85.4 keV, respectively. The intensity ratio of the Bi^{207} 570-keV γ rays to the K_α x rays was calculated semitheoretically. Experimental measurements that were used consisted of the Bi^{207} decay scheme established by Alburger and Sunyar,⁹ and the conversion coefficients measured by Ricci.¹⁰ Other quantities that enter into this calculation are the K -shell fluorescent yield,¹¹ the relative intensities of the K -x-ray components,¹¹ and the K/L capture ratio.¹² An intensity ratio $I_{570} : I_{K_\alpha} = 100 : (67 \pm 3)$ was calculated. The uncertainty includes estimated contributions from all the quantities listed above.

Several experimental checks were made on this ratio

⁸ D. Pelte, B. Povh, and W. Scholz, Nucl. Phys. **52**, 333 (1964); S. Buhl, D. Pelte, and B. Povh, *ibid.* **A91**, 319 (1967).

⁹ D. E. Alburger and A. W. Sunyar, Phys. Rev. **99**, 695 (1955).

¹⁰ R. A. Ricci, Physica **23**, 693 (1957).

¹¹ G. J. Nijgh, A. H. Wapstra, and R. Van Lieshout, *Nuclear Spectroscopy Tables* (North-Holland Publishing Company, Amsterdam, 1959).

¹² H. Brysk and M. E. Rose, Rev. Mod. Phys. **30**, 1169 (1958).

calculation for the Bi^{207} source used in this work. Firstly, the intensity ratio of the K_α to K_β x rays was measured using a lithium-drifted silicon detector which had a resolution (FWHM) for 74-keV x rays of 0.8 keV. The result for this ratio was 3.6 ± 0.2 , in good agreement with the expected¹¹ ratio of 3.40 ± 0.08 . Secondly, a relative efficiency curve was constructed from various radioactive sources for the 8-cc Ge(Li) detector used in the Mg^{22} work. From this efficiency curve, the Bi^{207} 570-keV γ ray to K_α x-ray intensity ratio was found to be $100:(61 \pm 8)$ in acceptable agreement with the calculated ratio given above.

For the measurements on Mg^{22} the target chamber consisted of a thin-walled glass bulb of ~ 3 -in. diameter having a re-entrant beam pipe and Ni window for admitting the beam to the gas volume. A 1-cm diam beam stopper, consisting of 0.002-in.-thick stainless steel foil, was held in place by a lead-through wire at a distance of 2 cm from the entrance window. Natural neon gas was admitted at a pressure of slightly less than 1 atm. The 8-cc Ge(Li) detector was placed close to the target chamber at 0° to the beam.

A mechanical beam chopper and electronic gating system¹³ was used, together with a He^{3++} beam of 6 MeV, to produce and count the radiations from the Mg^{22} activity. This device allowed a 1024-channel analyzer to store the spectrum only during a beam-off period of 12 msec, where the total irradiate-count cycle is 17 msec.

Initial runs on Mg^{22} revealed the presence of K_β x rays from lead which were presumably from room background. Iron shielding was therefore placed around the detector in order to reduce the intensities of these x rays.

The upper part of Fig. 5 shows the regions of the 74- and 583-keV lines in the Mg^{22} spectrum. For comparison purposes the target chamber was opened up, a Bi^{207} source was placed on the beam line midway between the entrance window and the beam stopper, and the glass bulb was remounted so that the absorption conditions would be nearly the same as for the Mg^{22} . The spectrum taken under these conditions is shown in the lower part of Fig. 5. Other runs were taken with the Bi^{207} source at various locations within the glass bulb and it was found that the spectra were all closely similar except for an additional 4% absorption of the x-ray lines when the source was located behind the beam stopper.

The calculation of the ratio $I_{74}:I_{583}$ for Mg^{22} was made by first finding the net areas in Fig. 5 under the 74- and 583-keV lines of Mg^{22} and under the K_α and 570-keV lines of Pb^{207} emitted by the Bi^{207} source. Because of the low-energy tails on the low-energy lines in Fig. 5, an arbitrary cutoff point was taken at channel 100 for Mg^{22} and at channel 101 for Bi^{207} . In the case of Bi^{207} the tail of the K_β line was assumed to be similar in

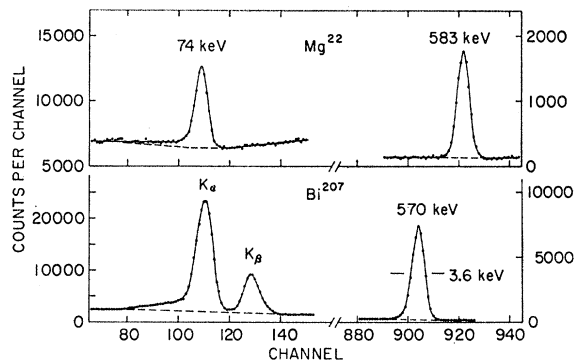


Fig. 5. Pulse-height spectra in an 8-cc Ge(Li) detector from Mg^{22} (upper curve) and Bi^{207} (lower curve) that were used for finding the intensity ratio of the 74- and 583-keV γ rays from Mg^{22} .

shape and relative amplitude to that of the K_α line, and its contribution was subtracted from the area under the K_α line.

The Mg^{22} spectrum in Fig. 5 shows slight evidence for a line at about channel 129, with ~ 1 –2% of the intensity of the 74-keV line, corresponding to $\text{Pb } K_\beta$ x rays not completely removed by the iron shielding around the Ge(Li) detector. Since the corresponding K_α line coincides with the Mg^{22} 74-keV line a correction of $(5 \pm 5)\%$ was subtracted from the net area under the 74-keV line to allow for the suspected presence of Pb x rays.

Among the several other small corrections was one of 2.6% for the difference in the efficiencies of the Ge(Li) detector for γ rays of 570 and 583 keV. The absolute efficiencies for detecting the 74-keV Mg^{22} line and the Bi^{207} K_α line were assumed to be equal.

The possibility was considered that the Mg^{22} activity, formed in a 3-mm diam by 2-cm long cylindrical column of the Ne gas between the entrance window and the beam stopper could diffuse outward with the result that some of the 74-keV γ rays would not have to pass through the 0.002-in. thick beam stopper to reach the detector. In such a case the effective absorption of the 74-keV γ rays would be different from that of the Bi^{207} K_α line of Fig. 5. This effect was studied by using a 0.005-in. thick Pt beam stopper with which it was found that $\sim \frac{1}{3}$ of the activity diffuses out and is detected in a position unshielded by the beam stopper. Since the total absorption of the 74-keV γ rays by the stainless steel beam stopper is 4%, a correction of 1% was made in the relative intensities of the 74-keV and K_α lines.

By using the experimental data on Bi^{207} , together with the previously quoted calculated ratio of the K_α and 570-keV lines for normalization, the following result on the γ -ray intensity ratio was obtained for Mg^{22}

$$I_{74}/I_{583} = 0.64 \pm 0.06.$$

This is to be compared with the corresponding ratio of 0.59 ± 0.02 obtained by Barker *et al.*⁵ Since all of the

¹³ D. E. Alburger, Phys. Rev. **131**, 1624 (1963).

γ rays from Mg^{22} are in cascade (see next section) and since there is no known positron branch to the ground state of Na^{22} , the above result corresponds to a value of $(36 \pm 6)\%$ for the positron branch to the 0.583-MeV level of Na^{22} .

B. Higher Levels of Na^{22}

Preliminary work at Strasbourg showed that the search for positron branches from Mg^{22} to states of Na^{22} above the 0.657-MeV level was obscured by the Na^{24} activity from the $Ne^{22}(He^3, p)Na^{24}$ reaction and so would benefit greatly from the use of an enriched Ne^{20} target rather than a natural neon target. Since neon gas enriched to 99.99% in Ne^{20} was available at Brookhaven National Laboratory,¹⁴ the search for decay to higher states was continued using the 3.5-MV electrostatic accelerator at that laboratory. The gas-target chamber used in this work was identical to that employed at Strasbourg except that the Ni foil entrance window was 0.00005 in. thick. The change to a thinner Ni window was made to increase the ratio of activities induced in the gas to those induced in the Ni foil since the latter activity was relatively strong (see Table II). A Ne gas pressure of ~ 1 atm was used. In addition, a liquid-air cold trap was placed near the gas target in order to minimize carbon build-up and the 8-cc Ge(Li) detector which was used was placed as close to the target as possible (~ 1 cm) and heavily shielded with lead. These steps resulted in a noticeable reduction in the background activities listed in Table II.

This investigation of $Mg^{22}(\beta^+)Na^{22}$ was carried out concurrently with an investigation of γ -ray transitions in Na^{22} induced by the $F^{19}(\alpha, n)Na^{22}$ and $Ne^{20}(He^3, p)Na^{22}$ reactions⁷ and thus the γ -ray decay modes of the Na^{22} states of interest and the corresponding transition energies were known. This was a great aid to the present work.

A total of eight Ge(Li) pulse-height spectra from $Mg^{22}(\beta^+)Na^{22}$ were recorded under different conditions. These were supplemented by spectra of the prompt radiations from $Ne^{20}+He^3$ and by background (both empty gas cell and beam off) spectra. From all these spectra one further γ -ray transition from $Mg^{22}(\beta^+)Na^{22}$ was identified as arising from feeding of the Na^{22} 1.937-MeV level. Upper limits were set on positron branches to all other Na^{22} levels with $E_x < 3.6$ MeV.

A portion of one of the Ge(Li) spectra from $Mg^{22}(\beta^+)Na^{22}$ is shown in Fig. 6. This spectrum was recorded with radioactive Bi^{207} and Co^{60} sources placed near the detector in order to provide an energy calibration. The full-energy-loss peaks of the two Co^{60} γ rays with energies¹⁵ of 1173.23 ± 0.04 and 1332.48 ± 0.05 keV are

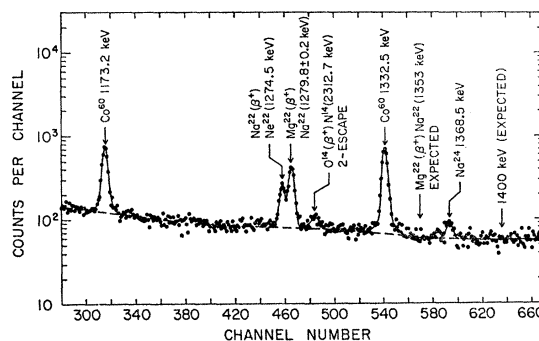


Fig. 6. Partial spectrum of γ rays from $Mg^{22}(\beta^+)Na^{22}$ obtained with an 8-cc Ge(Li) detector. The dispersion is 0.707 keV/channel and the energy resolution is 3.4-keV full-width-at-half-maximum. Co^{60} peaks arise from a radioactive source, the origin of the other peaks is discussed in the text. The curves are the results of least-squares fits to the data as described in the text.

identified in Fig. 6 as is the (1274.52 ± 0.07) -keV γ ray¹⁶ from $Na^{22}(\beta^+)Ne^{22}$. The latter arises from the $Ne^{20}(He^3, p)Na^{22}$ reaction as well as from the daughter activity in the decay $Mg^{22} \rightarrow Na^{22}$. Also apparent in Fig. 6 is the two-escape peak of the (2312.68 ± 0.10) -keV γ ray¹⁷ from $O^{14}(\beta^+)N^{14}$ which is produced via the $C^{12}(He^3, n)O^{14}$ reaction due to carbon contamination of the Ni foil and beam collimating system (see Table II). There is also evidence of a weak Na^{24} γ ray from $Na^{24}(\beta^-)Mg^{24}$. This γ ray was identified by its energy $(1368.53 \pm 0.04$ keV)¹⁵ and by the presence of the associated (2753.92 ± 0.12) -keV γ ray.¹⁵ The presence of these two Na^{24} γ rays was due to the small amount of Ne^{22} in the gas target (see Table I).

The γ ray with an energy of 1279.8 ± 0.2 keV is assigned to $Mg^{22}(\beta^+)Na^{22}$ for three reasons. First, its energy is in good agreement with the energy of 1280.5 ± 1.0 keV measured⁷ for the $Na^{22} 1.937 \rightarrow 0.657$ transition; second, its yield relative to that of the 0.583-MeV γ ray was found to be the same (within experimental errors of $\sim 10\%$) at two He^3 energies for which the $Ne^{20}(He^3, n)Mg^{22}(\beta^+)Na^{22}$ yield (Fig. 3) differed by a factor of 5; and third, it was not observed in background runs taken with the beam off or with the gas cell empty.

The data shown in Fig. 6 were taken to obtain an accurate energy for the Na^{22} 1280-keV γ ray. This was done by first determining the channel positions of the prominent γ rays by least-squares fits assuming Gaussian peaks superimposed on an exponential background (the solid and dashed curves of Fig. 6) and then determining the energies of the unknown γ -ray peaks relative to those from the Bi^{207} source (not shown) and the Co^{60} source. The energy of 1279.8 ± 0.2 keV for the $Na^{22} 1.937 \rightarrow 0.657$ γ ray results from the average of three such measurements taken under somewhat different conditions of amplifier bias and dispersion. We adopt

¹⁴ The enriched Ne^{20} gas was provided through the courtesy of Dr. A. J. Howard. See A. J. Howard and W. W. Watson, J. Chem. Phys. **40**, 1409 (1964).

¹⁵ G. Murray, R. L. Graham, and J. S. Geiger, Nucl. Phys. **63**, 353 (1965).

¹⁶ W. W. Black and R. L. Heath, Nucl. Phys. **A90**, 650 (1967).

¹⁷ C. Chasman, K. W. Jones, R. A. Ristinen, and D. E. Alburger, Phys. Rev. **159**, 830 (1967).

TABLE III. γ -ray branching ratios for the 1.937-MeV level of Na^{22} .

E_t (MeV)	E_γ (keV)	Branching ratio (%)
0	1936.9	<3
0.583	1353.8	<3
0.657	1279.9	100
0.891	1046.0	<4
1.528	408.8	<2

an energy of 1279.9 ± 0.2 keV for this γ ray based on an average of the present measurement with that of Ref. 7. It is clear from Fig. 6 that the good resolution (3.4-keV FWHM) of the 8-cc Ge(Li) detector used in this work was necessary in order to observe the Na^{22} 1280-keV γ ray in the presence of the Ne^{22} 1274.5-keV γ ray and the two-escape peak of the N^{14} 2312.7-keV γ ray.

The cascade to the 0.657-MeV level was the only γ -ray transition observed from the Na^{22} 1.937-MeV level. Intensity limits on γ -ray branches to other Na^{22} levels are given in Table III. This information came from spectra like those of Fig. 6 but with the Co^{60} and Bi^{207} sources removed. The expected position of the 1.354-MeV γ ray corresponding to the $1.937 \rightarrow 0.583$ transition is indicated in Fig. 6. Also indicated in Fig. 6 is the expected position of the 1400-keV γ ray corresponding to the Na^{22} $1.984 \rightarrow 0.583$ transition.⁷ The expected position of this γ ray is indicated to illustrate the type of information used to set upper limits on positron branches to other Na^{22} states. The upper limits obtained from these studies are listed in Table IV which summarizes our findings for the positron branching ratios in $\text{Mg}^{22}(\beta^+)\text{Na}^{22}$.

A value of $(5.1 \pm 0.4)\%$ for the positron branching ratio to the 1.937-MeV level was obtained from the relative intensities of the 583- and 1280-keV γ rays which were extracted from the spectra using a relative

efficiency curve for full-energy-loss peaks observed by the 8-cc Ge(Li) detector. Various radioactive sources were used to obtain this efficiency curve. The 511- and 1274-keV lines from radioactive Na^{22} were the most important for present purposes since these γ rays are close in energy to the 583- and 1280-keV lines from Mg^{22} . The same efficiency curve was used in setting the upper limits for positron branches to other states of Na^{22} (Table IV). The limits were set from the absence of the most intense γ ray emitted from a given level; however, due account was taken of other observed or possible γ -ray branches⁷ in converting limits on γ -ray relative intensities to limits on positron branching ratios.

The $\log ft$ values listed in Table IV were calculated (computer) using the method of Feenberg and Trigg.¹⁸

C. The 0.657-MeV Level

From the above result on the decay of Mg^{22} to the 1.937-MeV level, together with the measured intensity ratio of the 74- and 583-keV γ rays derived previously, the branch to the 0.657-MeV level is calculated to be $(59 \pm 6)\%$. Although this branch has the same value as that obtained by Barker *et al.*⁵ it should be pointed out that the correction for the branch to the 1.937-MeV level would reduce the result of Barker *et al.*, who did not observe this branch, to $(53.9 \pm 2.1)\%$.

IV. PRECISION ENERGY MEASUREMENTS

A. The 74-keV γ Ray in Mg^{22} Decay

The energy of the 74-keV γ ray in the decay of Mg^{22} was measured by recording the Mg^{22} spectrum when a source of Ti^{44} was superposed. The latter activity emits γ rays having energies¹⁹ of 67.85 ± 0.04 keV and 78.38 ± 0.04 keV. After suitably adjusting the position of this source with respect to the detector, pulse-height

TABLE IV. Branching ratios in $\text{Mg}^{22}(\beta^+)\text{Na}^{22}$.

Na^{22} level ^a (keV)	$J^\pi; T$	Prominent γ ray (keV)	β^+ end-point energy ^b (MeV)	β^+ intensity (%)	$\log ft$
583.05 ± 0.1	$1^+; 0$	583	3.230	36 ± 6^c	3.74 ± 0.08
657.0 ± 0.14	$0^+; 1$	583, 74	3.156	59 ± 6^c	3.49 ± 0.05
890.9 ± 0.2	$4^+; 0$	891	2.922	<0.29	>5.6
1528.1 ± 0.3	$5^+; 0$	1528	2.285	<0.12	>5.5
1936.9 ± 0.23	$1^+; 0$	1280	1.876	5.1 ± 0.4	3.55 ± 0.04
1951.8 ± 0.3	$2; 1$	1369	1.861	<0.25	>4.8
1983.5 ± 0.5	$2^+, 3^+; (0)$	1400	1.829	<0.16	>5.0
2211.4 ± 0.32	$1^-; (0)$	1554	1.602	<0.3	>4.4
2571.5 ± 0.3	$1, 2; (0)$	2572	1.241	<0.3	>4.0
2968.6 ± 0.6	$3; 0$	1017	0.844	<0.25	>3.3
3059.4 ± 0.6	$2; 0$	1108	0.754	<0.2	>3.2
3527 ± 7.0	≥ 2	1575	0.286	<0.35	>1.2

^a The data listed in the first three columns are from Ref. 7 with the exception of present results for the 1.937-MeV level.

^b All β^+ end-point energies have uncertainties of 20 keV because of the uncertainty in the mass of Mg^{22} (see Ref. 6). This uncertainty contributes to those in the $\log ft$ values.

^c The % branches to the 0.583- and 0.657-MeV levels sum to $(94.9 \pm 0.4)\%$ assuming no other branches except that to the 1.937-MeV level.

¹⁸ E. Feenberg and G. Trigg, Rev. Mod. Phys. **22**, 399 (1950).

¹⁹ R. A. Ristinen and A. W. Sunyar, Phys. Rev. **153**, 1209 (1967).

spectra were obtained consisting of a well-resolved triplet, where the 74-keV Mg^{22} line was approximately midway between the two Ti^{44} lines. Over-all linearity was checked with a precision pulser. Computer fits were made to the data. The average from two runs is 73.9 ± 0.1 keV for the energy of the Mg^{22} γ ray.

B. The 472-keV γ Ray in the Decay of Na^{24m}

A measurement incidental to the study of Mg^{22} decay was a determination of the energy of the 472-keV γ ray emitted from the 19.6-msec isomeric state² of Na^{24} . As mentioned in connection with Fig. 2 this state is excited in the $Ne^{22}(He^3, p)Na^{24}$ reaction. For this purpose a source of Ir^{192} was superposed. This activity emits a number of γ rays whose energies are known with very high accuracy; one of these has an energy of 468.050 ± 0.016 keV.²⁰ In the spectrum of the combined sources the Ir line forms a resolved doublet with the 472-keV Na^{24} line. The 511-keV annihilation line was used to find the dispersion of the spectrum. Based on a computer fit to the data the energy of the Na^{24} γ ray is 472.3 ± 0.1 keV.

V. DISCUSSION

We have found a half-life of 4.03 ± 0.05 sec for the ground state of Mg^{22} . This is in agreement with previous results.^{1,3,5} The weighted average of these previous results with the present one is 4.00 ± 0.04 sec. We use this weighted average in the calculations described in this section.

The positron branching ratios listed in Table IV are also consistent with previous results.^{1,3,5} A mass excess of $-(347 \pm 20)$ keV⁶ (C^{12} scale) for Mg^{22} was used to calculate the $\log ft$ values listed in Table IV. For the positron transition to the 0^+ , $T=1$ 0.657-MeV level (Table IV) the $\log ft$ value of 3.49 ± 0.05 is consistent with the value of 3.49 expected for a $0^+ \rightarrow 0^+$ super-allowed transition. However, the branching ratio of this transition must be determined with considerably greater accuracy before such a comparison becomes informative.

The $\log ft$ value for the positron decay to the 1.937-

MeV level is seen to be allowed. Thus, this level has $J^\pi=1^+$, $J=0$ being forbidden by its γ -ray decay to the 0^+ 0.657-MeV level. The Gamow-Teller matrix element of the positron transition between the $J^\pi=0^+$, $T=1$ Mg^{22} ground state and the $J^\pi=1^+$, $T=0$ Na^{22} 1.937-MeV level is related to the $M1$ transition between the 1.937-MeV level and the $J^\pi=0^+$, $T=1$ 0.657-MeV level of Na^{22} , since the 0^+ states differ only in T_z . The Gamow-Teller matrix element has a spin part only. The $M1$ matrix element contains a spin part, which is proportional to the Gamow-Teller matrix element, and a space part. For $\log ft \lesssim 3.5$ the spin part of the $M1$ matrix element is expected to be considerably larger than the space part.²¹ Neglecting the space part, and using the relation between the Gamow-Teller and $M1$ matrix elements given by Kurath,²¹ we find that the mean lifetime of the Na^{22} 1.937 \rightarrow 0.657 transition corresponding to the $\log ft$ value of Table IV is $\tau = (2.4 \pm 0.3) \times 10^{-14}$ sec. This is consistent with the limit $\tau < 6 \times 10^{-14}$ sec obtained via the Doppler shift attenuation method.⁷

Using the same method of comparison for the 0.657 \rightarrow 0.583 γ -ray transition, we find that the upper limit reported² for the mean lifetime of the Na^{22} 0.657-MeV level, $\tau < 5 \times 10^{-10}$ sec, is consistent with the $\log ft$ value of the positron decay to the 0.583-MeV level (Table IV) which corresponds to $\tau = (6.6 \pm 1.2) \times 10^{-11}$ sec if the space part of the $M1$ matrix element is neglected. It may be possible to infer something about the magnitudes and relative phases of the space and spin parts of these two $M1$ matrix elements when the $\log ft$ values are more accurately known and the speeds of the γ -ray transitions are measured.

ACKNOWLEDGMENTS

We are indebted to A. W. Sunyar for suggesting the use of the Bi^{207} comparison and for the loan of the Ti^{44} source, and to E. der Mateosian for the use of the high-resolution silicon detector system for the measurements on Bi^{207} . We wish to thank W. R. Phillips for informing us of the results of the Manchester group on Mg^{22} prior to publication and for informative communications.

²⁰ J. B. Marion, Technical Report 656 (unpublished).

²¹ D. Kurath, Argonne National Laboratory Report ANL-7108 1965, p. 61 (unpublished).